

# Reduced methionine synthase expression results in uracil accumulation in mitochondrial DNA and impaired oxidative capacity

Katarina E. Heyden<sup>a</sup>, Joanna L. Fiddler<sup>a</sup>, Yuwen Xiu<sup>a</sup>, Olga V. Malysheva<sup>a</sup>, Michal K. Handzlik<sup>b</sup>, Whitney N. Phinney<sup>c</sup>, Linsey Stiles<sup>d</sup>, Sally P. Stabler<sup>c</sup>, Christian M. Metallo<sup>b,e</sup>, Marie A. Caudill<sup>a</sup> and Martha S. Field<sup>b,a,\*</sup>

<sup>a</sup>Division of Nutritional Sciences, Cornell University, Ithaca, NY 14853, USA

<sup>b</sup>Department of Bioengineering, University of California, La Jolla, San Diego, CA 92093, USA

<sup>c</sup>Department of Medicine, University of Colorado, Aurora, CO 80217, USA

<sup>d</sup>Department of Medicine/Division of Endocrinology, University of California, Los Angeles, CA 90095, USA

<sup>e</sup>Molecular and Cell Biology Laboratory, Salk Institute for Biological Studies, La Jolla, CA 92037, USA

\*To whom correspondence should be addressed: Email: [mas246@cornell.edu](mailto:mas246@cornell.edu)

Edited By: Patrick Stover

## Abstract

Adequate thymidylate [deoxythymidine monophosphate (dTMP) or the “T” base in DNA] levels are essential for stability of mitochondrial DNA (mtDNA) and nuclear DNA (nDNA). Folate and vitamin B12 (B12) are essential cofactors in folate-mediated one-carbon metabolism (FOCM), a metabolic network which supports synthesis of nucleotides (including dTMP) and methionine. Perturbations in FOCM impair dTMP synthesis, causing misincorporation of uracil (or a “U” base) into DNA. During B12 deficiency, cellular folate accumulates as 5-methyltetrahydrofolate (5-methyl-THF), limiting nucleotide synthesis. The purpose of this study was to determine how reduced levels of the B12-dependent enzyme methionine synthase (MTR) and dietary folate interact to affect mtDNA integrity and mitochondrial function in mouse liver. Folate accumulation, uracil levels, mtDNA content, and oxidative phosphorylation capacity were measured in male  $Mtr^{+/+}$  and  $Mtr^{+/-}$  mice weaned onto either a folate-sufficient control (C) diet (2 mg/kg folic acid) or a folate-deficient (FD) diet (lacking folic acid) for 7 weeks.  $Mtr$  heterozygosity led to increased liver 5-methyl-THF levels.  $Mtr^{+/-}$  mice consuming the C diet also exhibited a 40-fold increase in uracil in liver mtDNA.  $Mtr^{+/-}$  mice consuming the FD diet exhibited less uracil accumulation in liver mtDNA as compared to  $Mtr^{+/+}$  mice consuming the FD diet. Furthermore,  $Mtr^{+/-}$  mice exhibited 25% lower liver mtDNA content and a 20% lower maximal oxygen consumption rates. Impairments in mitochondrial FOCM are known to lead to increased uracil in mtDNA. This study demonstrates that impaired cytosolic dTMP synthesis, induced by decreased  $Mtr$  expression, also leads to increased uracil in mtDNA.

**Keywords:** methionine synthase, folate, vitamin B12, DNA, uracil

## Significance Statement

The relationship between folate and vitamin B12 (B12) in supporting nucleotide synthesis for nuclear DNA replication has been recognized for decades. This study demonstrates that either reduced expression of the B12-dependent enzyme methionine synthase ( $Mtr$ ) or exposure to a folate-deficient (FD) diet caused uracil accumulation in mtDNA; decreased  $Mtr$  expression also impaired oxidative capacity (a biomarker of mitochondrial function). Moreover, uracil accumulation in mtDNA in  $Mtr^{+/-}$  mice consuming the FD diet was attenuated relative to  $Mtr^{+/+}$  mice consuming the FD diet. This finding provides a possible mechanistic explanation underlying recent observational studies that have raised concerns over associations of negative health outcomes with the combination of low B12 status and increasing folate exposure.

## Introduction

Vitamin B12 (B12) deficiency disproportionately impacts older adults, vegans/vegetarians, and pregnant women (1). Hematological and neurological symptoms are typical of B12 deficiency, due to the role of B12 in DNA synthesis. B12 and folate (vitamin B9) are essential cofactors required for folate-mediated

one-carbon metabolism (FOCM), a metabolic pathway which provides one-carbon groups for de novo biosynthesis of nucleotides and methyl donor generation (1). Only two mammalian enzymes require B12 as a cofactor: methylmalonyl CoA mutase (MCM), which supports metabolism of amino acids and fatty acids through the tricarboxylic acid cycle and resides in the

**Competing Interest:** The authors declare no competing interest.

**Received:** December 21, 2022. **Revised:** March 16, 2023. **Accepted:** March 21, 2023

© The Author(s) 2023. Published by Oxford University Press on behalf of National Academy of Sciences. This is an Open Access article distributed under the terms of the Creative Commons Attribution-NonCommercial-NoDerivs licence (<https://creativecommons.org/licenses/by-nc-nd/4.0/>), which permits non-commercial reproduction and distribution of the work, in any medium, provided the original work is not altered or transformed in any way, and that the work is properly cited. For commercial re-use, please contact [journals.permissions@oup.com](mailto:journals.permissions@oup.com)

mitochondria, and methionine synthase (MTR), which is part of FOCM and localizes to the cytosol (1).

MTR uses both folate and B12 cofactors to catalyze regeneration of methionine from homocysteine. In this two-step process, 5-methyltetrahydrofolate (5-methyl-THF) donates a methyl group to cobalamin (a form of B12), releasing THF and generating methylcobalamin (2). Methylcobalamin then provides the methyl group to homocysteine for methionine synthesis (2). The conversion of 5,10-methylene-THF to 5-methyl-THF by methylenetetrahydrofolate reductase (MTHFR) is irreversible, and the only enzyme capable of metabolizing 5-methyl-THF to release THF is MTR (3) (Fig. 1). Without adequate B12 levels or as a result of decreased MTR levels, folate becomes increasingly trapped in the 5-methyl-THF form, which decreases the availability of other folate cofactors (i.e. THF and 5,10-methylene-THF) for key processes such as nucleotide synthesis. Therefore, a hallmark of B12 deficiency is the cellular accumulation of 5-methyl-THF, a phenomenon commonly known as the “5-methyl trap” (3).

As mentioned above, folate is required for synthesis of thymidylate [deoxythymidine monophosphate (dTMP), or the “T” base in DNA]. dTMP is a precursor of deoxythymidine triphosphate (dTTP). dTTP is unique among DNA bases, as DNA polymerases incorrectly incorporate a uracil (or “U”) base into DNA when dTTP levels are low (4). Uracil misincorporation leads to activation of base-excision repair mechanisms, which, in the continued absence of dTMP, lead to DNA double-strand breaks, stalled replication fork progression, and DNA instability (4). Folate-dependent dTMP synthesis occurs in multiple cellular compartments (cytosol, nucleus, and mitochondria) (5, 6). There is evidence that either dietary or genetic FOCM impairments decrease cytosolic and nuclear dTMP synthesis leading to nuclear DNA (nDNA) instability (5).

Mitochondrial DNA (mtDNA) is relatively small (16.5 kb) and circular in structure, making it distinct from nDNA. mtDNA encodes for components of the protein complexes within the mitochondrial membrane that allow for energy production through oxidative phosphorylation (OXPHOS) (7). mtDNA replication is one component of mitochondrial biogenesis, and maintenance of mtDNA is closely tied to mitochondrial function (7). Nucleotide synthesis, specifically de novo dTMP synthesis, has been shown to occur in the mitochondria and to be essential for maintaining mtDNA integrity (6). Evidence in cultured cells (8) and mouse liver (9) suggests mtDNA is more sensitive than nDNA to dietary folate deficiency. The effects of impaired B12 deficiency on mtDNA stability are almost completely uncharacterized.

The folate–B12 interrelationship has received increased attention, as observational data in humans have associated the combination of elevated folate status with low or deficient B12 status (known as “high folate/low B12”) with a wide array of negative health outcomes: worsened clinical markers of B12 deficiency, diminished response to B12 treatment, and increased risk for cognitive impairment and decline among the elderly (10, 11). However, there are little data from B12-deficient model systems investigating the molecular mechanisms underlying these associations. This study used genetic disruption of the B12-dependent *Mtr* enzyme in mice (12). Decreased *Mtr* expression perturbed cellular folate distribution, caused uracil accumulation in liver mtDNA, decreased liver mtDNA content, and reduced mitochondrial respiratory capacity in the liver. The increased uracil in mtDNA was attenuated in *Mtr*<sup>+/-</sup> mice (relative to *Mtr*<sup>+/+</sup> mice) exposed to folate-deficient (FD) diets. These data provide one of the first mechanistic explanations linking a biomarker of

low B12 status, increasing folate exposure, and an adverse physiological outcome.

## Results

### Reduced *Mtr* expression alters whole liver folate distribution but does not affect total folate concentrations

*Mtr*<sup>+/+</sup> and *Mtr*<sup>+/-</sup> mice were weaned onto either control (C; AIN93G-based diet with 2 mg/kg folic acid) or FD (AIN93G-based diet lacking folic acid) diet and maintained on these defined diets for 7 weeks until sacrifice. Mice on the FD diet had slightly higher overall food intake than those on C diet ( $P < 0.01$ ), though there were no differences in mouse body weight between groups (Fig. S1A and B). Liver MTR protein levels were reduced by 60% ( $P < 0.001$ ) in *Mtr*<sup>+/-</sup> mice consuming the C diet (Fig. 2A). Interestingly, liver MTR protein levels were also reduced ( $P < 0.001$  for effect of diet) as a result of FD diet exposure (Fig. 2A). The same diet and genotype effects were also observed in the kidney tissue ( $P = 0.04$  and  $P = 0.018$ , respectively; Fig. S2).

Folate deficiency and reduced *Mtr* expression elicited changes in plasma transmethylation metabolite levels (Table 1). As previously observed (13), changes in transmethylation biomarkers were observed with FD diet exposure, which increased homocysteine ( $P = 0.018$ ), cystathionine ( $P < 0.0001$ ), and methylglycine ( $P = 0.023$ ) and decreased cysteine ( $P = 0.052$ ) and  $\alpha$ -aminobutyric acid ( $P = 0.02$ ; Table 1). *Mtr*<sup>+/-</sup> genotype-driven changes were observed in methionine and methylglycine levels ( $P = 0.046$  and  $P < 0.001$ , respectively; Table 1). As expected, plasma folate was lower with FD diet exposure ( $P < 0.0001$ ; Table 1). In addition, *Mtr*<sup>+/-</sup> genotype did not impact plasma folate accumulation, in agreement with previous findings in this model (14). As anticipated, plasma MMA was unaffected by either *Mtr*<sup>+/-</sup> genotype or folate deficiency (Table 1), indicating that B12-dependent methylmalonyl-CoA mutase enzyme activity was not affected in the *Mtr*<sup>+/-</sup> model (i.e. the model is specific to the B12-dependent enzymatic activity involved in FOCM).

Exposure to the FD diet reduced total liver folate levels of both *Mtr*<sup>+/+</sup> and *Mtr*<sup>+/-</sup> mice by 50% when measured by liquid chromatography-mass spectrometry (LC–MS) ( $P < 0.0001$ ; Fig. 1B) and microbiological assay ( $P = 0.014$ ; Fig. S3). *Mtr* genotype did not influence total liver folate accumulation (Figs. 2B and S3). One-carbon metabolism consists of several one-carbon substituted folate forms to serve as cofactors and dietary vitamin B12 deficiency is associated with accumulation of folate as 5-methyl-THF; therefore, folate cofactor distribution was quantified. In mice consuming the C diet, reduced *Mtr* expression increased the amount of whole-cell liver 5-methyl-THF from 33 to 43% of total folate ( $P = 0.02$ ), with corresponding changes in the percentage of folates from THF ( $P = 0.038$ ) and formyl-THF ( $P < 0.001$ ) (Fig. 2C and D). These changes in folate distribution support the presence of a more subtle 5-methyl-THF trap in *Mtr*<sup>+/-</sup> mice than in other models of B12 deficiency in which 5-methyl-THF levels are elevated 2- to 3-fold (15). 5-Methyl-THF accumulation was normalized in *Mtr*<sup>+/-</sup> mice consuming the FD diet (Fig. 2C and D). Interestingly, the amount of liver folate in the form of folic acid was very low, accounting for  $< 0.01\%$  of all folates even in mice consuming the C diet (Fig. 2F). This suggests that folic acid does not appreciably accumulate in the liver of mice consuming defined diets containing 2 mg/kg folic acid.

Total folate levels in liver mitochondria were 20% ( $P = 0.03$ ) lower in mice consuming the FD diet (Fig. 3A), as assessed by LC–MS analysis and confirmed by *Lactobacillus casei* microbiological assay

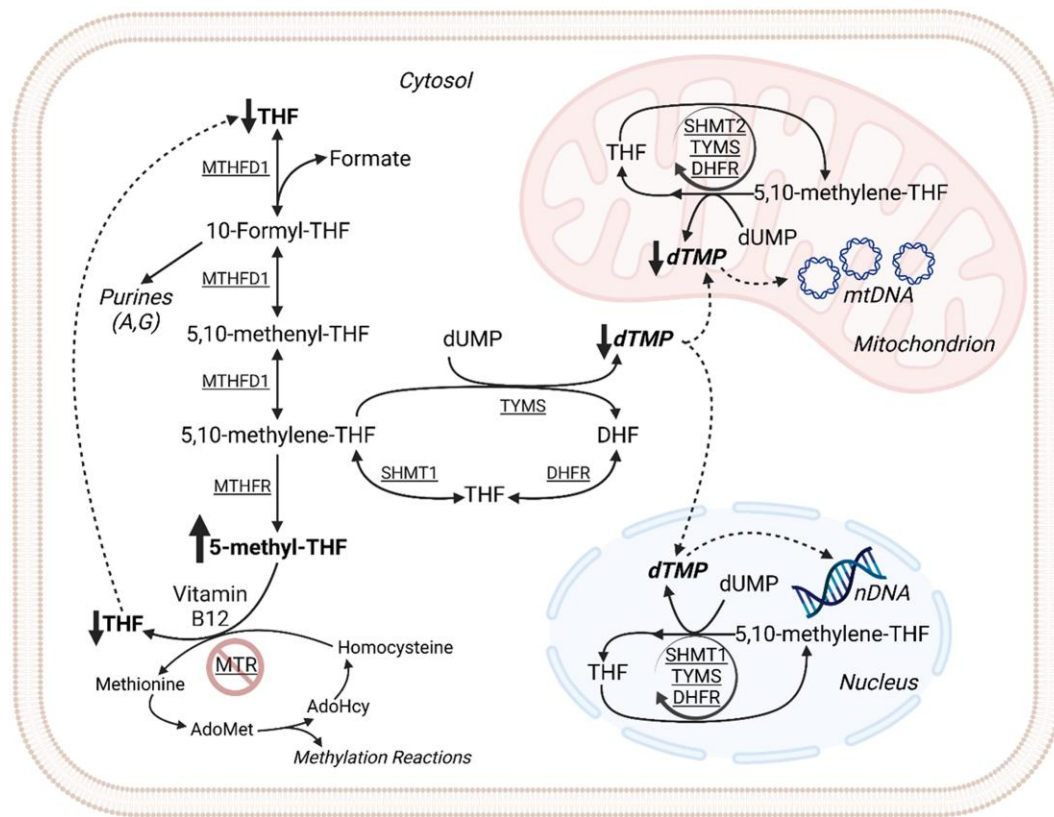


**Fig. 1.** The effects of decreased *Mtr* expression on FOCM. Vitamin B12 deficiency, as modeled by partial knockout of the *Mtr* gene in mice, causes elevation of cellular folate as 5-methyl-THF and matched reduction of folate as THF. The conversion of 5,10-methylene-THF to 5-methyl-THF is irreversible, and 5-methyl-THF can only be metabolized to THF by the MTR enzyme using B12 as a cofactor. Created at biorender.com. AdoHcy, S-adenosylhomocysteine; AdoMet, S-adenosylmethionine; DHFR, dihydrofolate reductase; dTMP, deoxythymidine monophosphate; dUMP, deoxyuridine monophosphate; FOCM, folate-mediated one-carbon metabolism; MTHFD1, methylenetetrahydrofolate dehydrogenase 1; MTHFR, methylenetetrahydrofolate reductase; MTR, methionine synthase; mtDNA, mitochondrial DNA; nDNA, nuclear DNA; SHMT, serine hydroxymethyltransferase; THF, tetrahydrofolate; TYMS, thymidylate synthase.

( $P = 0.01$ ; Fig. S3). As with whole-cell liver folate levels, *Mtr* genotype did not impact total folate levels in liver mitochondria (Fig. 3A). The primary form of folate detected in liver mitochondrial fractions was THF, which consisted of >90% of mitochondrial folates (Fig. 3B) and was consistent with previous literature (16, 17). While *Mtr*<sup>+/-</sup> genotype altered 5-methyl-THF levels in liver mitochondria of mice on C diet ( $P < 0.0001$ ; Fig. 3C), this increase from 2 to 4% may not be biologically meaningful. There was no detectable level of folic acid present in liver mitochondria.

### ***Mtr* genotype leads to uracil misincorporation in mtDNA and impaired mitochondrial function**

We recently developed an assay to quantify uracil misincorporation into mtDNA (9). As described in detail above, uracil misincorporation arises when de novo dTMP synthesis is impaired by either folate or B12 deficiency (5, 18). To assess whether the altered whole-cell folate distribution with *Mtr* loss could affect mtDNA integrity, uracil content of liver mtDNA was measured by quantitative real-time PCR assay (9). In liver mitochondria, there was a significant interaction between diet and genotype for mtDNA uracil accumulation ( $P = 0.0001$ ; Fig. 4A). Compared to *Mtr*<sup>+/+</sup> mice consuming the C diet, both reduced *Mtr* expression ( $P < 0.001$ ) and folate deficiency ( $P < 0.001$ ) were associated with uracil accumulation in liver mtDNA (Fig. 4A). Uracil levels in mtDNA were elevated nearly 40-fold in *Mtr*<sup>+/-</sup> mice compared to *Mtr*<sup>+/+</sup> mice consuming the C diet (Fig. 4A). *Mtr*<sup>+/-</sup> mice consuming

the FD diet exhibited lower uracil in liver mtDNA relative to FD *Mtr*<sup>+/+</sup> mice ( $P = 0.0001$ ; Fig. 4A), suggesting a protective effect against uracil accumulation in mtDNA in this experimental group. As observed previously (9), uracil was not randomly distributed throughout the mitochondrial genome but was enriched in specific regions of mtDNA (Fig. S4). Importantly, uracil accumulation observed in liver mtDNA with reduced *Mtr* expression or exposure to the FD diet was not observed in liver nDNA (Fig. S5), as observed in other models (9). These data suggest that the 5-methyl-THF trap in whole cell liver causes a disturbance in the cytosolic folate pool and leads to uracil misincorporation to mtDNA in mice consuming adequate dietary folate (C diet). Exposure to the FD diet attenuates both the whole-cell 5-methyl-THF accumulation (Fig. 2D) and uracil accumulation in mtDNA (Fig. 4A), suggesting that the decrease in whole-cell 5-methyl-THF levels induced by FD diet also decreases uracil in mtDNA.

In addition to investigating the integrity of mtDNA, we also quantified mtDNA content, which is increasingly recognized as an indicator of mitochondrial dysfunction (7, 19). Reduced *Mtr* expression was associated with a 25% decrease in mtDNA content in mouse liver ( $P = 0.045$ ; Fig. 4B). This observed decrease was not due to a decrease in mitochondrial mass in *Mtr*<sup>+/-</sup> liver samples, as there was no difference in citrate synthase activity between groups (Fig. 4C).

To understand the effects of reduced *Mtr* expression on mitochondrial oxidative capacity, maximal respiratory complex

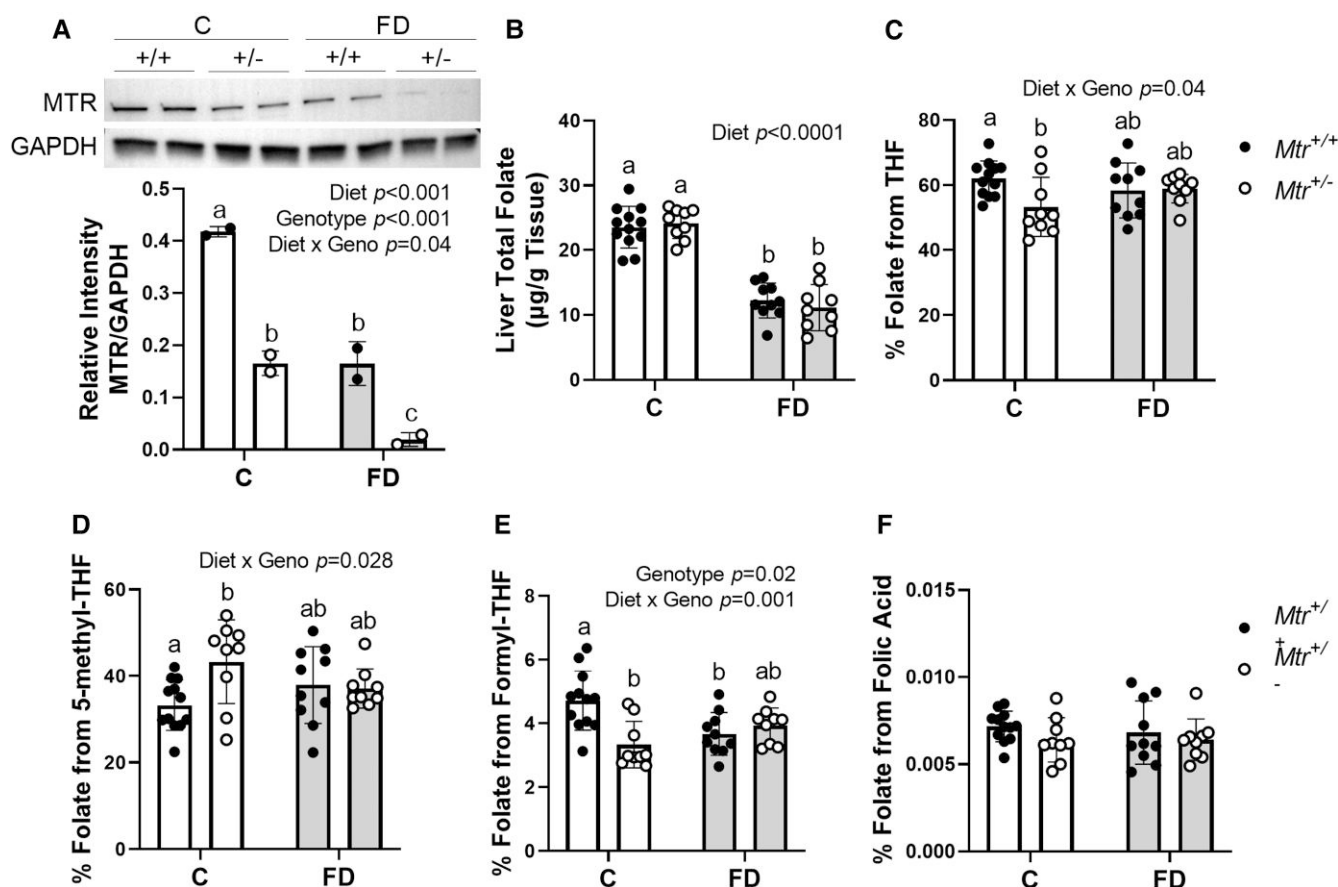


**Fig. 2.** MTR protein expression and folate distribution in *Mtr*<sup>+/+</sup> and *Mtr*<sup>+/-</sup> liver. A) Liver MTR protein levels normalized to GAPDH; *n* = 2 per group. B) Total liver folate; *n* = 9–12 per group. C) Liver folate distribution from THF; *n* = 9–12 per group. D) Liver folate distribution from 5-methyl-THF; *n* = 9–12 per group. E) Liver folate distribution from formyl-THF; *n* = 9–12 per group. F) Liver folate distribution from folic acid; *n* = 9–12 per group. Folate distribution was quantified using LC-MS/MS. Two-way ANOVA with Tukey's post hoc analysis was used to assess main effects of diet and genotype and diet-genotype interaction. Data are presented as mean ± SD with statistical significance defined *P* ≤ 0.05. Groups not connected by a common letter are significantly different. C, control diet; FD, folate-deficient diet; GAPDH, glyceraldehyde-3-phosphate dehydrogenase; MTR, methionine synthase; THF, tetrahydrofolate.

**Table 1.** Plasma metabolite profile for *Mtr*<sup>+/+</sup> and *Mtr*<sup>+/-</sup> mice.

Metabolite	Control (C) diet		Folate-deficient (FD) diet		P-value of model effect		
	<i>Mtr</i> <sup>+/+</sup>	<i>Mtr</i> <sup>+/-</sup>	<i>Mtr</i> <sup>+/+</sup>	<i>Mtr</i> <sup>+/-</sup>	Diet	Genotype	Diet × genotype
Folate (ng/mL)	177.7 ± 80.5	170.5 ± 48.9	25.3 ± 17.3	30 ± 26.9	<0.0001	ns	ns
Methylmalonic acid (µM)	1.5 ± 0.3	1.6 ± 0.2	1.7 ± 0.1	1.6 ± 0.2	ns	ns	ns
Homocysteine (µM)	6.4 ± 1.2	7.2 ± 0.7	13.6 ± 11.1	19.2 ± 12.2	0.018	ns	ns
Cystathionine (nM)	1,134.9 ± 316.4	1,000.7 ± 162.7	1,740 ± 348.1	1,663.6 ± 438.6	<0.001	ns	ns
Cysteine (µM)	263 ± 27.6	255 ± 21.9	243 ± 33.7	226.6 ± 16.2	0.052	ns	ns
α-Aminobutyric acid (µM)	19.9 ± 5.5	18.5 ± 4.5	15.2 ± 3.9	14.4 ± 2.7	0.02	ns	ns
Methionine (µM)	51.9 ± 6.9	49.6 ± 4	49.6 ± 6.3	42.1 ± 4.1	ns	0.046	ns
Glycine (µM)	270.7 ± 52	261 ± 32.3	235.5 ± 38.7	271.6 ± 43.8	ns	ns	ns
Serine (µM)	106 ± 13.3	103.5 ± 7.3	108.3 ± 11.7	105.8 ± 16.2	ns	ns	ns
Dimethylglycine (µM)	10.8 ± 1.7	11.3 ± 2.1	11.2 ± 2.1	9.4 ± 1.1	ns	ns	ns
Methylglycine (µM)	7.9 ± 2.4	57.1 ± 3.6	45.1 ± 26.3	55 ± 13.8	0.023	<0.001	0.012

Folate concentration was measured using *L. casei* microbiological assay. MMA concentration was measured by GC-MS. All other biomarkers were measured via stable isotope dilution capillary GC-MS. Data were analyzed by two-way ANOVA with Tukey's post hoc analysis for diet and genotype main effects and diet-genotype interaction. Data are presented as mean ± SD with statistical significance defined as *P* ≤ 0.05; *n* = 4–8 per group. ns, not significant.

activity was measured in the liver. There were no changes in activity of complex I or complex II with *Mtr* loss or FD diet exposure (Fig. 4D and E). Interestingly, reduced *Mtr* expression decreased the activity of complex IV by 20% (*P* = 0.026; Fig. 4F), suggesting that reduced *Mtr* expression impairs mitochondrial oxidative capacity.

## Discussion

In this study, the *Mtr*<sup>+/-</sup> mouse model was used to determine how cytosolic 5-methyl-THF accumulation (one biomarker of B12 deficiency) affected mtDNA integrity and mitochondrial function. As mentioned earlier, B12 is required by only two enzymes: MTR and

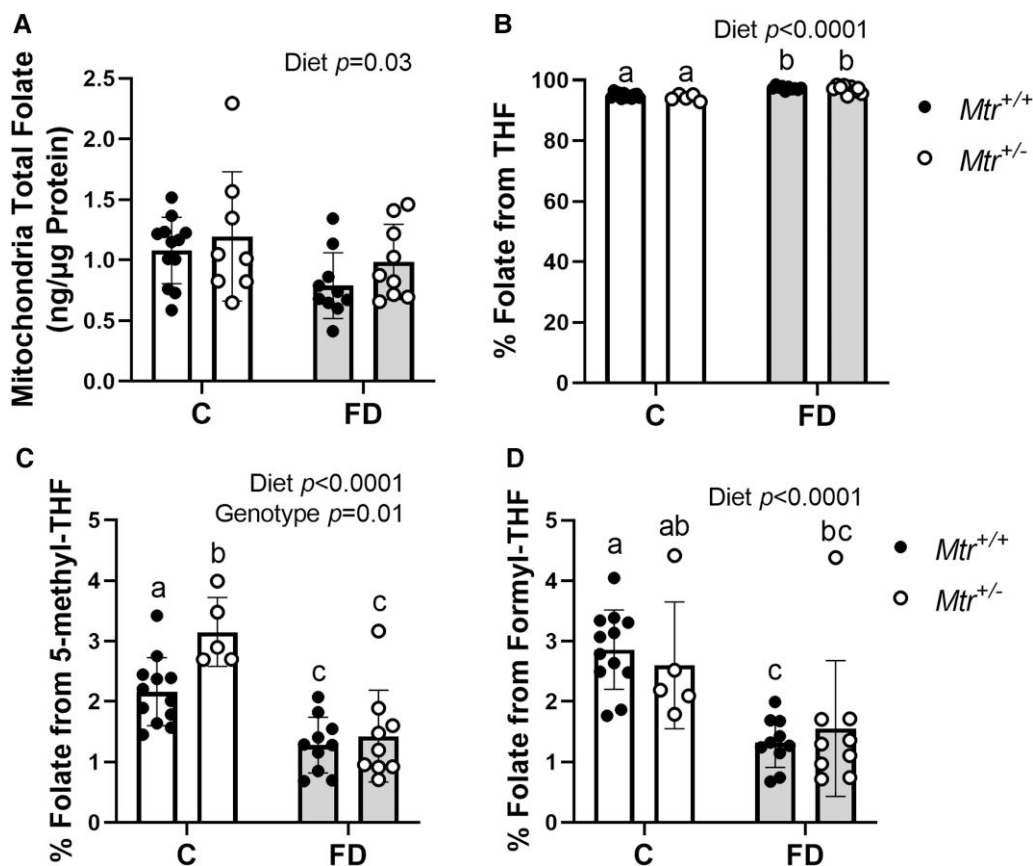


**Fig. 3.** Total folate and folate distribution in mitochondrial fraction from  $Mtr^{+/+}$  and  $Mtr^{+/-}$  liver. A) Total mitochondrial folate;  $n=9-12$  per group. B) Folate distribution from THF;  $n=9-12$  per group. C) Folate distribution from 5-methyl-THF;  $n=9-12$  per group. D) Folate distribution from 5-formyl-THF;  $n=9-12$  per group. Folate distribution was quantified using LC-MS/MS. Data are shown as mean  $\pm$  SD. Two-way ANOVA with Tukey's post hoc analysis was used to assess main effects of diet and genotype and diet-genotype interaction with statistical significance defined as  $P \leq 0.05$ . Groups not connected by a common letter are significantly different. C, control diet; FD, folate-deficient diet; Mtr, methionine synthase; THF, tetrahydrofolate.

MCM. Elevated MMA, a by-product of excess MCM substrate, is a classical marker to diagnose B12 deficiency. The  $Mtr^{+/-}$  mouse model does not exhibit altered plasma MMA levels (Table 1), meaning that the model recapitulates one effect of B12 deficiency that is specific to impaired FOCM.

Decreased *Mtr* expression shifted liver whole-cell folate distribution to modestly elevate 5-methyl-THF levels at the expense of THF levels (Fig. 2C and D). The majority of total cellular folate is distributed evenly between the cytosolic and mitochondrial compartments (with about 10% in the nuclear compartment) (20). Reduced *Mtr* expression did not notably alter mitochondrial folate distribution (Fig. 3B-D). Therefore, the changes observed in whole-cell folate distribution are likely underestimating the true accumulation of 5-methyl-THF in the cytosolic compartment as a result of reduced *Mtr* expression. It is equally important to note that the increase in 5-methyl-THF in  $Mtr^{+/-}$  mice occurred even in the presence of sufficient dietary B12 levels.

As described earlier, an accumulation of 5-methyl-THF decreases folate cofactors needed for nucleotide biosynthesis, impairing de novo dTMP synthesis and DNA replication and/or repair (3). The observation that uracil in mtDNA is elevated in  $Mtr^{+/-}$  mice (Fig. 4A) suggests that the mitochondrial compartment is sensitive to changes in cytosolic de novo dTMP synthesis capacity and/or that a cytosolic 5-methyl-trap decreases the amount of cytosolic dTMP available for transport to the mitochondria. Mitochondrial dTMP synthesis capacity has been shown to be insufficient to maintain adequate mitochondrial dTMP levels and

prevent mtDNA uracil misincorporation in cell culture models (8). In addition, 5-methyl-THF is a tight-binding inhibitor of the enzyme serine hydroxymethyltransferase 1 (SHMT1), which is essential for de novo dTMP synthesis (Fig. 1) (5, 21), providing a second mechanism whereby 5-methyl-THF accumulation may impair cytosolic dTMP synthesis contributing to uracil accumulation in mtDNA (Fig. 3A).

The phenotype of uracil accumulation in this model was specific to mtDNA, as uracil levels in nDNA remained unchanged (Fig. S5), consistent with our previous findings in the *Shmt2*<sup>+/-</sup> mouse model (9) and in other models employing the same FD and length of dietary exposure (22). Taken together, these data suggest that mtDNA is more sensitive to impaired FOCM than is nDNA or that mtDNA uracil may be an earlier biomarker of FOCM dysfunction. In addition, uracil levels in nDNA vary widely by tissue type (5). Studies are needed to determine whether mtDNA uracil levels also vary by tissue type and whether uracil can be detected in lymphocyte DNA, which would facilitate its use as a biomarker.

Recent advances in next-generation DNA sequencing technology have also revealed that uracil is more likely to be incorporated at specific loci within nDNA (23, 24), and this is believed to be modified by replication timing and/or heterochromatic state. mtDNA uracil was also not randomly distributed throughout the mitochondrial genome (Fig. S4), consistent with what was observed previously (9). Although the molecular mechanisms underlying region-specific patterns of uracil incorporation in

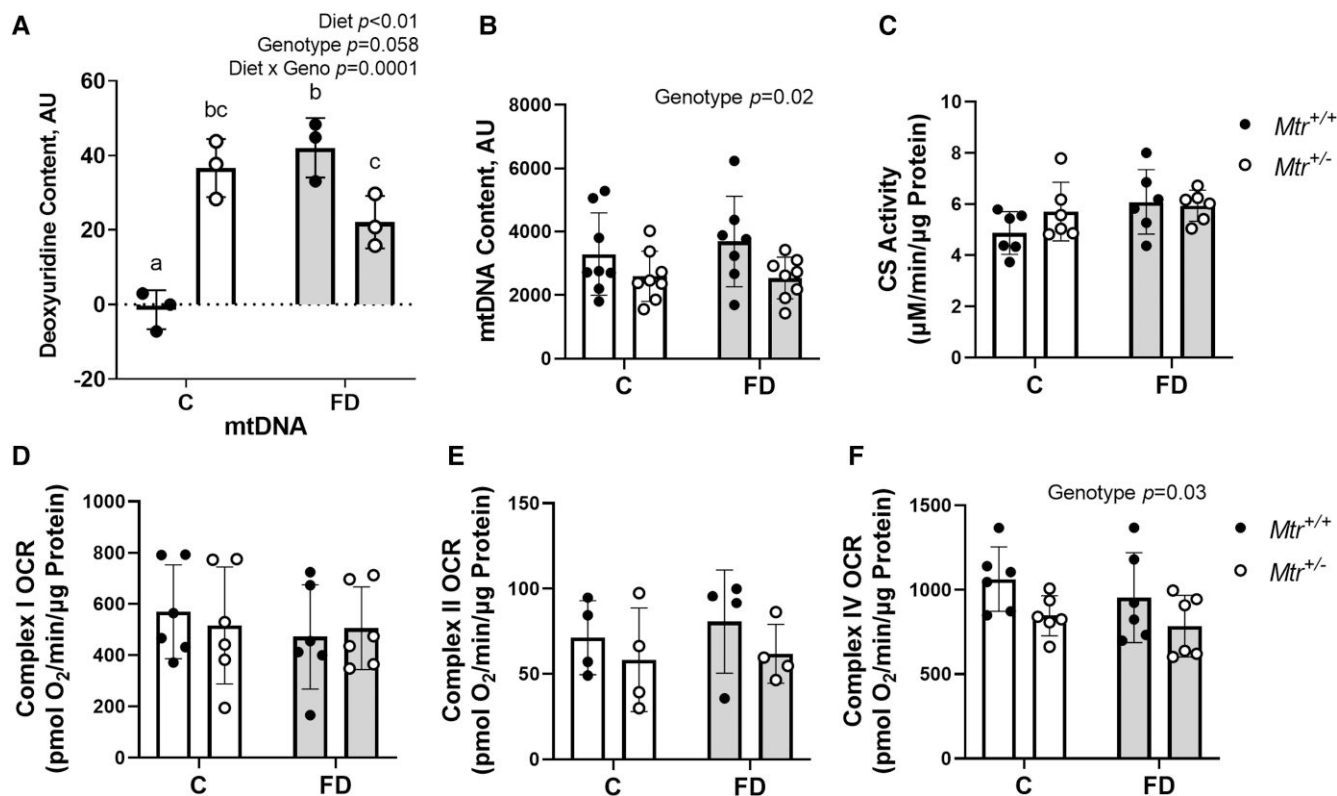


**Fig. 4.** Biomarkers of impaired mitochondrial one-carbon metabolism. A) Uracil content in liver mitochondrial DNA;  $n = 3$  per group. B) mtDNA copy number in liver determined using real-time PCR;  $n = 6$  per group. C) Mitochondrial mass quantified using citrate synthase activity in the liver;  $n = 6$  per group. Data are shown as mean  $\pm$  SD and were analyzed by two-way ANOVA with Tukey's post hoc analysis, with significance defined as  $P \leq 0.05$ . Groups not connected by a common letter are significantly different. AU, arbitrary units; C, control diet; CS, citrate synthase; FD, folate-deficient diet; Mtr, methionine synthase; OCR, oxygen consumption rate.

mtDNA have not been identified, there is some overlap between uracil-enriched regions and common mouse mtDNA deletion loci (25).

The physiological consequences of uracil accumulation in mtDNA have not yet been fully investigated, nor is it clear to which level uracil must accumulate to become detrimental to mitochondrial function. Decreased *Shmt2* expression impairs mitochondrial FOCM and also causes uracil accumulation in liver mtDNA (9). Decreased *Shmt2* did not affect liver mtDNA content or liver mitochondrial mass (9). Importantly, uracil accumulation in the *Shmt2*<sup>+/-</sup> model closely paralleled impairments in OXPHOS and mitochondrial membrane potential (9). Uracil accumulation in liver mtDNA as a result of disrupted cytosolic FOCM (i.e. decreased *Mtr* expression) (Fig. 4A) was also associated with impaired maximal complex IV oxidative capacity (Fig. 4F), which has been shown to be the regulatory center for liver OXPHOS capacity and which is essential for liver function (26, 27). However, reduced *Mtr* expression also led to decreased mtDNA content in the liver (Fig. 4B), suggesting an additional means by which *Mtr*<sup>+/-</sup> genotype may perturb mitochondrial function.

As described above, the combination of elevated folate status with low or deficient B12 status is associated with a wide array of negative health outcomes, though mechanisms have not been thoroughly investigated in model systems (10). This study presents evidence of an adverse molecular phenotype (i.e. increased uracil accumulation in mtDNA) resulting from the combination of reduced expression of a B12-dependent enzyme and folate exposure, as mtDNA uracil levels were lower in *Mtr*<sup>+/-</sup> mice consuming the FD diet than in *Mtr*<sup>+/+</sup> mice consuming the FD diet. This finding is

compelling because mitochondrial function changes are associated with many of the pathologies identified in the observational literature as a result of B12 deficiency that appear to be exacerbated by increasing folate and/or folic acid exposures. Further studies using a more extensive range of dietary folic acid content and/or more pronounced dietary B12 deficiency are needed to more fully elucidate these mechanisms and to determine the utility of mtDNA uracil as a biomarker of risk for adverse pathologies.

## Materials and methods

### Breeding of *Mtr*<sup>+/+</sup> and *Mtr*<sup>+/-</sup> mice

The *Mtr*<sup>+/-</sup> mouse model, generated as previously described (12), was backcrossed for more than 10 generations to C57Bl/6J. To characterize the interaction between reduced *Mtr* expression and varying levels of dietary folic acid exposure, C57Bl/6J females were intercrossed with *Mtr*<sup>+/-</sup> males. Male *Mtr*<sup>+/+</sup> and *Mtr*<sup>+/-</sup> offspring were then weaned and randomly assigned to one of two defined diets at 3 weeks of age. The diets consisted of defined AIN93G C diet containing 2 mg/kg folic acid (#117814GI; Dyets, Inc., Bethlehem, PA, USA), or an AIN93G-based FD diet lacking folic acid (#117815GI; Dyets, Inc., Bethlehem, PA, USA)  $n = 20$ –25 mice per group. Dietary intake and body weight were recorded every 14 days. Mice were maintained on these diets for 7 weeks and sacrificed via cervical dislocation following CO<sub>2</sub> euthanasia. Mice were fasted for 12 h prior to harvest. Whole blood was collected via cardiac puncture into heparin-coated tubes, and plasma and red blood cells were separated by centrifugation at 2,500 $\times$ g in a

microcentrifuge tube and immediately flash frozen in liquid nitrogen. Tissues were harvested, rinsed in ice-cold 1× phosphate-buffered saline (PBS, Corning), and immediately flash frozen in liquid nitrogen or used for liver mitochondrial isolation (described below). Plasma, red blood cells, and tissues were then stored at  $-80^{\circ}\text{C}$  for further analysis.

### Mitochondrial isolation

Mitochondria were isolated from fresh mouse liver as previously described (9). Mitochondria were saved as pellets or resuspended in extraction buffer [2% (wt/vol) sodium ascorbate, 0.2 M beta-mercaptoethanol, 0.05 M HEPES pH 7.85, 0.05 M CHES pH 7.85] to prevent folate degradation. Samples were stored at  $-80^{\circ}\text{C}$ .

### Folate distribution

Folate levels and vitamer distribution for liver and mitochondrial samples were quantified by LC–electrospray tandem MS adapted from previously described methods (28–31). Liver and mitochondrial samples were weighed at the time of harvest. Liver total folate levels were normalized to liver weight. Mitochondrial total folate levels were normalized to protein concentration, which was assessed by Lowry–Bensadoun assay (32).

### Lactobacillus casei assay for total folates

Liver tissue, liver mitochondria (stored in extraction buffer), and plasma folate concentrations were measured by the microbiological *L. casei* assay as previously described (33). *Lactobacillus casei* growth was quantified at 550 nm by Epoch Microplate Spectrophotometer (Biotek Instruments). Total folate measurements for liver and purified liver mitochondria were normalized to protein concentrations for each sample.

### Uracil in mtDNA measured by real-time PCR

DNA was isolated from frozen mitochondrial pellets using a QIAprep Spin Miniprep Kit (Qiagen). Uracil in mtDNA was quantified using a previously described real-time PCR assay (9).

### Uracil in nDNA measured using GC–MS

DNA was isolated using High Pure PCR Template Preparation Kit (Roche). Following RNase A treatment, DNA was purified using High Pure PCR Purification Kit (Roche), and concentrations were quantified by Qubit (Thermo Scientific). Two micrograms of DNA was treated with uracil DNA glycosylase (UDG, New England Biolabs, Inc.) for 60 min at  $37^{\circ}\text{C}$  with gentle shaking. Samples were derivatized and uracil levels quantified as previously described (9).

### mtDNA copy number qPCR

DNA from liver and cell pellets was isolated using High Pure PCR Template Preparation Kit (Roche). DNA concentrations were measured by Nanodrop 2000c Spectrophotometer (Thermo Scientific). Quantitative PCR to measure mtDNA content was performed as previously described (34).

### Mitochondrial mass

Mitochondrial mass in whole liver was measured according to the manufacturer's instructions using the Citrate Synthase Activity Assay Kit (Sigma) and normalized to protein concentration. Protein concentrations were assessed by Lowry–Bensadoun assay (32). Absorbance of the colorimetric assay was quantified by Epoch Microplate Spectrophotometer (Biotek Instruments).

### Respirometry in frozen samples

The oxygen consumption rate (OCR) of liver mitochondria was measured using the Seahorse XFe24 Extracellular Flux Analyzer (Agilent Technologies) as previously described (35) with minor modifications. Briefly, mitochondria from frozen liver were isolated in ice-cold MAS buffer using a Potter–Elvehjem (Teflon-glass) homogenizer with 10 strokes followed by centrifugation. Protein concentrations of the liver mitochondria supernatant were determined by a Pierce BCA Protein Assay (Thermo Fisher). Mitochondrial homogenates (150  $\mu\text{g}$ ) were loaded into the assay plates and centrifuged at  $2,000\times g$  for 5 min at  $4^{\circ}\text{C}$  with no brake. The OCR of each complex was determined using Wave software (Agilent) and was defined by the highest respiratory capacity value following the injection of the corresponding complex stimulating substrate: complex I, NADH; complex II, succinate; and complex IV, TMPD.

### Plasma metabolite analysis

Total plasma folate was assessed by *L. casei* assay as mentioned above. Total plasma levels of homocysteine, cystathionine, cysteine,  $\alpha$ -aminobutyric acid, methionine, glycine, serine, dimethylglycine, and methylglycine were quantified by stable isotope dilution capillary gas chromatography–mass spectrometry (GC–MS) as previously described (36, 37). MMA quantification was performed using 3  $\mu\text{L}$  of plasma that was spiked with [U- $^{13}\text{C}$ ]–MMA (Cambridge Isotope Laboratories, cat# CLM-9426-PK) as previously described (38) using GC–MS.

### Immunoblotting

Tissues were lysed by sonication in lysis buffer (150 mM NaCl, 10 mM Tris–Cl, 5 mM EDTA pH 8, 5 mM dithiothreitol, 1% Triton X-100, protease inhibitor), and cell debris was removed by centrifugation at  $4^{\circ}\text{C}$  for 10 min at  $14,000\times g$ . Protein concentrations of tissue or cell lysate supernatants were assessed by Lowry–Bensadoun assay (32). Samples were boiled with SDS–PAGE sample loading buffer (6× SDS), and 30  $\mu\text{g}$  of protein was loaded to each well of a 10% Tris–glycine SDS–PAGE gel (BioRad). Proteins were transferred to a PVDF membrane (Millipore). Membranes were blocked with 5% (wt/vol) nonfat dry milk in 1× PBS with 0.05% Tween-20 for 1 h. Membranes were then incubated for 1 h with 1:2,000 primary antibody [glyceraldehyde-3-phosphate dehydrogenase (GAPDH), Cell Signaling #14C10;  $\alpha$ -MTR, ProteinTech #25896] in 5% bovine serum albumin (BSA) 0.02%  $\text{NaN}_3$ . Membranes were then washed three times in 1× PBS with 0.01% Tween-20 and incubated for 1 h with HRP-conjugated secondary antibody diluted 1:20,000 in 5% (wt/vol) nonfat dry milk in 1× PBS with 0.05% Tween-20. Membranes were exposed with chemiluminescent substrate (BioRad) and visualized using a ProteinSimple Imager (Bio-technique). Protein levels were quantified using ImageJ software.

### Statistical analyses

All statistical analyses were performed with R statistical software (version 4.0.4 “Lost Library Book”). Experiments comparing two genotypes (*Mtr*<sup>+/+,+/-</sup>) and two different diets (C/FD) were analyzed using a two-way ANOVA with fixed effects of genotype, diet, and genotype–diet interaction and were followed by Tukey's post hoc analysis. Body weight and food intake data sets were analyzed using a two-way ANOVA with mixed effects of diet and time. Model assumptions of normality and homogenous variance for each data set were confirmed by QQ plot and Levene's test, respectively. Data are presented as means  $\pm$  standard deviation.

## Acknowledgments

The authors acknowledge assistance with statistical analysis from the Cornell Statistical Consulting Unit. This manuscript was posted as a preprint on bioRxiv, doi: <https://doi.org/10.1101/2022.08.29.505750>.

## Supplementary material

Supplementary material is available at PNAS Nexus online.

## Funding

The authors also acknowledge the National Defense Science and Engineering Graduate Fellowship program for funding support.

## Author contributions

K.E.H. and M.S.F. designed research; K.E.H., J.L.F., Y.X., O.V.M., W.N.P., L.S., S.S.S., M.K.H., C.M.M., and M.A.C. performed research; K.E.H. analyzed data; K.E.H. and M.S.F. wrote the paper.

## Data availability

All data are available in the main text or in the supplementary materials.

## References

- Green R, et al. 2017. Vitamin B12 deficiency. *Nat Rev Dis Primer*. 3: 17040.
- Nielsen MJ, Rasmussen MR, Andersen CBF, Nexø E, Moestrup SK. 2012. Vitamin B12 transport from food to the body's cells—a sophisticated, multistep pathway. *Nat Rev Gastroenterol Hepatol*. 9: 345–354.
- Shane B, Stokstad ELR. 1985. Vitamin B12-folate interrelationships. *Annu Rev Nutr*. 5:115–141.
- Chon J, Field MS, Stover PJ. 2019. Deoxyuracil in DNA and disease: genomic signal or managed situation? *DNA Repair (Amst)*. 77: 36–44.
- Field MS, Kamynina E, Chon J, Stover PJ. 2018. Nuclear folate metabolism. *Annu Rev Nutr*. 38:219–243.
- Anderson DD, Quintero CM, Stover PJ. 2011. Identification of a de novo thymidylate biosynthesis pathway in mammalian mitochondria. *Proc Natl Acad Sci*. 108:15163–15168.
- Gilkerson R. 2017. The little big genome the organization of mitochondrial DNA. *Front Biosci*. 22:710–721.
- Alonzo JR, Venkataraman C, Field MS, Stover PJ. 2018. The mitochondrial inner membrane protein MPV17 prevents uracil accumulation in mitochondrial DNA. *J Biol Chem*. 293:20285–20294.
- Fiddler JL, et al. 2021. Reduced Shmt2 expression impairs mitochondrial folate accumulation and respiration, and leads to uracil accumulation in mouse mitochondrial DNA. *J Nutr*. 151: 2882–2893.
- Maruvada P, et al. 2020. Knowledge gaps in understanding the metabolic and clinical effects of excess folates/folic acid: a summary, and perspectives, from an NIH workshop. *Am J Clin Nutr*. 112:1390–1403.
- Molloy AM. 2020. Adverse effects on cognition caused by combined low vitamin B-12 and high folate status—we must do better than a definite maybe! *Am J Clin Nutr*. 112:1422–1423.
- Swanson DA, et al. 2001. Targeted disruption of the methionine synthase gene in mice. *Mol Cell Biol*. 21:1058–1065.
- MacFarlane AJ, et al. 2008. Cytoplasmic serine hydroxymethyltransferase regulates the metabolic partitioning of methylenetetrahydrofolate but is not essential in mice. *J Biol Chem*. 283: 25846–25853.
- Dayal S, et al. 2005. Cerebral vascular dysfunction in methionine synthase-deficient mice. *Circulation*. 112:737–744.
- Palmer AM, Kamynina E, Field MS, Stover PJ. 2017. Folate rescues vitamin B12 depletion-induced inhibition of nuclear thymidylate biosynthesis and genome instability. *Proc Natl Acad Sci U S A*. 114: E4095–E4102.
- Horne DW, Patterson D, Cook RJ. 1989. Effect of nitrous oxide inactivation of vitamin B12-dependent methionine synthetase on the subcellular distribution of folate coenzymes in rat liver. *Arch Biochem Biophys*. 270:729–733.
- Tibbetts AS, Appling DR. 2010. Compartmentalization of mammalian folate-mediated one-carbon metabolism. *Annu Rev Nutr*. 30:57–81.
- Xiu Y, Field MS. 2020. The roles of mitochondrial folate metabolism in supporting mitochondrial DNA synthesis, oxidative phosphorylation, and cellular function. *Curr Dev Nutr*. 4:nzaa153.
- Castellani CA, Longchamps RJ, Sun J, Guallar E, Arking DE. 2020. Thinking outside the nucleus: mitochondrial DNA copy number in health and disease. *Mitochondrion* 53:214–223.
- Lan X, Field MS, Stover PJ. 2018. Cell cycle regulation of folate-mediated one-carbon metabolism. *WIREs Syst Biol Med*. 10:e1426.
- Misselbeck K, Marchetti L, Priami C, Stover PJ, Field MS. 2019. The 5-formyltetrahydrofolate futile cycle reduces pathway stochasticity in an extended hybrid-stochastic model of folate-mediated one-carbon metabolism. *Sci Rep*. 9:4322.
- Beaudin AE, et al. 2012. Dietary folate, but not choline, modifies neural tube defect risk in Shmt1 knockout mice12345. *Am J Clin Nutr*. 95:109–114.
- Shu X, et al. 2018. Genome-wide mapping reveals that deoxyuridine is enriched in the human centromeric DNA. *Nat Chem Biol*. 14:680–687.
- Pálinkás HL, et al. 2020. Genome-wide alterations of uracil distribution patterns in human DNA upon chemotherapeutic treatments. *eLife* 9:e60498.
- Damas J, Carneiro J, Amorim A, Pereira F. 2014. Mitobreak: the mitochondrial DNA breakpoints database. *Nucleic Acids Res*. 42: D1261–D1268.
- Kadenbach B. 2021. Complex IV—the regulatory center of mitochondrial oxidative phosphorylation. *Mitochondrion* 58:296–302.
- Lesner NP, et al. 2022. Differential requirements for mitochondrial electron transport chain components in the adult murine liver. *eLife*. 11:e80919.
- Vishnumohan S, Arcot J, Pickford R. 2011. Naturally-occurring folates in foods: method development and analysis using liquid chromatography–tandem mass spectrometry (LC–MS/MS). *Food Chem*. 125:736–742.
- Freisleben A, Schieberle P, Rychlik M. 2003. Specific and sensitive quantification of folate vitamins in foods by stable isotope dilution assays using high-performance liquid chromatography–tandem mass spectrometry. *Anal Bioanal Chem*. 376:149–156.
- West AA, et al. 2012. Folate-status response to a controlled folate intake in nonpregnant, pregnant, and lactating women. *Am J Clin Nutr*. 96:789–800.
- Pfeiffer CM, Fazili Z, McCoy L, Zhang M, Gunter EW. 2004. Determination of folate vitamins in human serum by stable-isotope-dilution tandem mass spectrometry and comparison with radioassay and microbiologic assay. *Clin Chem*. 50: 423–432.

- 32 Bensadoun A, Weinstein D. 1976. Assay of proteins in the presence of interfering materials. *Anal Biochem.* 70:241–250.
- 33 Suh JR, Oppenheim EW, Girgis S, Stover PJ. 2000. Purification and properties of a folate-catabolizing enzyme. *J Biol Chem.* 275: 35646–35655.
- 34 Malik AN, Czajka A, Cunningham P. 2016. Accurate quantification of mouse mitochondrial DNA without co-amplification of nuclear mitochondrial insertion sequences. *Mitochondrion* 29: 59–64.
- 35 Acin-Perez R, et al. 2020. A novel approach to measure mitochondrial respiration in frozen biological samples. *EMBO J.* 39: e104073.
- 36 Allen RH, Stabler SP, Lindenbaum J, Serum betaine N. 1993. N-Dimethylglycine and N-methylglycine levels in patients with cobalamin and folate deficiency and related inborn errors of metabolism. *Metab Clin Exp.* 42:1448–1460.
- 37 Stabler SP, Lindenbaum J, Savage DG, Allen RH. 1993. Elevation of serum cystathionine levels in patients with cobalamin and folate deficiency. *Blood* 81:3404–3413.
- 38 Cordes T, Metallo CM. 2019. Quantifying intermediary metabolism and lipogenesis in cultured mammalian cells using stable isotope tracing and mass spectrometry. In: D'Alessandro A, editors. *High-throughput metabolomics: methods and protocols, methods in molecular biology.* Clifton, NJ: Springer. p. 219–241.